Inorganic Chemistry

Article

pubs.acs.org/IC

Uranium(IV) Sulfates: Investigating Structural Periodicity in the Tetravalent Actinides

David D. Schnaars and Richard E. Wilson*

Heavy Elements and Separation Sciences Group, Chemical Sciences and Engineering Division, Argonne National Laboratory, Argonne, Illinois 60439

Supporting Information

ABSTRACT: Chemical trends within the periodic table are frequently used as guides for predicting reactivity, structure, and electronic properties of the elements. While these trends have been rigorously investigated for the transition metals, the understanding of trends within the actinide series is elementary in comparison. Herein, we report the synthesis and characterization of five new U(IV) sulfate compounds and discuss their relationship to previously reported An(IV) sulfate species, an analysis that allows for the elucidation of solid state trends across the actinides. One such trend suggests the increase in Lewis acidity that occurs when traversing the actinides from thorium to plutonium promotes bidentate binding of the sulfate ligand as long as complexation can outcompete the resulting increase in steric pressure. This hypothesis correlates well with the experimental results previously reported for the solution phase speciation in An(IV) sulfate systems.

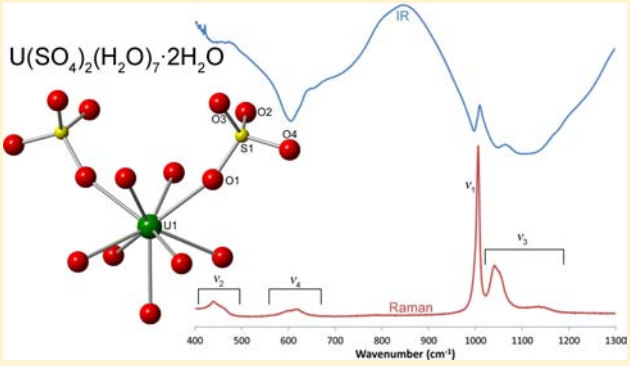

INTRODUCTION

Chemical trends have been used as coarse guides for predicting reactivity, structure, and electronic properties of the elements since the modern form of the periodic table was first proposed by Mendeleev. For example, the concept of chemical periodicity was critical to placement of both the 4f lanthanide and 5f actinide elements in the Periodic Table. The periodic decrease in the metal−ligand bond length observed in structural studies of the binary tetravalent oxides and halides of the actinides allowed Seaborg to propose his actinide hypothesis, which placed the 5f elements where they currently reside in the Periodic Table.[1−3] Additionally, fundamental electronic differences between the actinides and lanthanides were deduced from an ion-exchange study of the trivalent ions, indicating that the 5f orbitals of the An(III) ions allow for greater complexation of chloride due to their increased ability to participate in bonding interactions in comparison to the 4f orbitals of the Ln(III) ions.[4] Finally, the progressive filling of the 5f orbitals within the actinide series results in the well-known actinide contraction. The actinide contraction is responsible for the periodic increase in the Lewis acidity and hardness of the tetravalent actinide ions from Th (the softest) to Pu. In aqueous solution, this contraction results in an increase in the Bronsted acidities of the aquated tetravalent cations, as well the increasing thermodynamic stability of An(IV) coordination complexes with strong donor ligands.[5−8]

Inspired by trends in structure and reactivity observed in the series of binary halides and oxides across the actinides, we are interested in exploring more complex ligand systems such as sulfate. We chose the sulfate system because it is a polyprotic and polydentate ligand that can exhibit a variety of coordination modes both in solution and the solid state.[9,10] The energetics of different coordination geometries and stabilities have been shown by Wipff et al. to be on the order of the energetics required for a chemical separation of two isovalent metal ions.[11] Therefore, we are interested in studying the structural changes in actinide coordination chemistry not only from the fundamental view of chemical periodicity, but also as a potentially important variable in understanding metal-ion separations.

The solution phase speciation and ligand binding of An(IV) sulfates was recently explored by Hennig and colleagues, where they reported a change in the preferential sulfate binding mode from monodentate to bidentate when traversing the actinides from Th to Np.[12−14] More recently, we reported a study looking at the coordination of sulfate to Pu(IV) in aqueous solution.[10] Our findings agree with the trend identified by Hennig and show a predominance of bidentate sulfate coordination to Pu(IV), a result we ascribed to the increased Lewis acidity of Pu(IV) versus the earlier An(IV) ions. While these studies show a trend in coordination geometry across the actinides in solution, our previously reported structural analysis of Pu(IV) sulfate complexes demonstrated the difficulty of correlating this trend to the solid state due in part to the lack of

Received: June 18, 2012
Published: August 21, 2012

dx.doi.org/10.1021/ic301291w | Inorg. Chem. 2012, 51, 9481−9490

Table 1. X-ray Crystallographic Data for Complexes 1, 2, 3, 4, and 5

	1	2	3	4	5
empirical formula	$H_{18}O_{17}S_2U$	$H_{10}O_{13}S_2U$	$H_6K_4O_{19}S_4U$	$H_{2.5}O_{17.25}Rb_4S_4U$	$Cs_2H_4O_{14}S_3U$
crystal habit, color	block, green	irregular, green	block, green	irregular, green	plate, green
crystal size (mm)	0.16 × 0.10 × 0.10	0.10 × 0.06 × 0.06	0.23 × 0.18 × 0.14	0.14 × 0.14 × 0.09	0.05 × 0.05 × 0.02
crystal system	monoclinic	orthorhombic	monoclinic	monoclinic	monoclinic
space group	$P2_1/m$	$Pnma$	$P2_1/c$	$P2_1/c$	$P2_1/c$
volume (Å^3)	681.66(16)	915.2(3)	1739.4(5)	1786.8(4)	1322.5(4)
a (Å)	7.1755(10)	14.624(3)	12.4184(19)	12.4780(16)	6.4674(11)
b (Å)	12.0865(16)	11.093(2)	11.1585(17)	11.3264(15)	12.782(2)
c (Å)	7.9343(11)	5.6416(11)	13.512(2)	13.4294(18)	16.366(3)
α (deg)	90	90	90	90	90
β (deg)	97.853(2)	90	111.721(2)	109.705(2)	102.182(6)
γ (deg)	90	90	90	90	90
Z	2	4	4	4	4
formula weight (g/mol)	592.29	520.23	832.72	986.67	828.06
density (calculated) (Mg/m^3)	2.886	3.776	3.180	3.668	4.159
absorption coefficient (mm^{-1})	12.302	18.266	10.866	20.458	18.243
F_{000}	556	952	1560	1778	1464
total no. reflections	2669	12418	29117	28484	15987
unique reflections	2669	1398	6551	6066	3051
final R indices [$I > 2\sigma(I)$]	R_1 = 0.0273, wR_2 = 0.0726	R_1 = 0.0324, wR_2 = 0.0876	R_1 = 0.0330, wR_2 = 0.0809	R_1 = 0.0380, wR_2 = 0.0736	R_1 = 0.0370, wR_2 = 0.0754
largest diff peak and hole (e$^-$ Å^{-3})	2.842 and −1.854	3.216 and −2.840	3.318 and −1.616	1.738 and −1.423	1.760 and −1.431
GOF	1.067	1.108	1.050	0.991	1.006

structurally characterized An(IV) sulfate compounds and the diversity of complexes which may be synthesized.[15]

To date, the literature contains 20 An(IV) sulfate complexes characterized by single crystal X-ray diffractometry where SO_4^{2-} is the only anion. Of these 20 compounds, 7 contain thorium,[16−23] 4 contain neptunium,[24−27] 6 contain plutonium,[15,28] and only 3 contain uranium.[13,18,29] The dearth of uranium compounds may be attributed to the redox instability of aqueous U(IV), which readily oxidizes to U(VI) forming the uranyl dication, UO_2^{2+}, in aqueous solution. The overall lack of structurally characterized U(IV) sulfate species highlights a need for additional study of this system in order to elucidate the chemical trends and properties across the entire An(IV) sulfate series.

Herein, we present the synthesis, single crystal structures, and vibrational spectra of four new U(IV) sulfate complexes, three of which are charge balanced using alkali metal cations. Additionally, we also present the solid state structure for a new hydration state of the neutral U(IV) sulfate β-phase previously reported by Kierkegaard.[29] The solid state structures of these compounds are compared to previously reported An(IV) sulfate species as a part of a periodic ensemble of complexes.

EXPERIMENTAL SECTION

Caution: Depleted uranium is an alpha-emitting radionuclide and standard precautions for handling radioactive materials should be observed when performing the following synthetic procedures.

All reactions were performed under aerobic conditions. To help inhibit oxidation of U(IV) to U(VI) during crystal growth, the solutions were stored and crystallized under an atmosphere of nitrogen. All materials were obtained from commercial sources and used as received.

$U(SO_4)_2(H_2O)_7{\cdot}2H_2O$ (1). A yellow solution of 0.5 m uranium and 2.0 m H_2SO_4 was prepared by dissolving 576 mg (2.0 mmol) of UO_3 into 444 μL (8.0 mmol) of conc. H_2SO_4 and 3.935 mL of H_2O. The uranium was subsequently reduced using a two electrode cell over several hours to form a green solution of pure U(IV) as confirmed by UV−vis spectroscopy. The addition of 20 mL of ethanol to the solution resulted in the deposition of a green solid. After centrifugation, the pale yellow solution was decanted off and the green solid was washed with an additional 20 mL of ethanol before being isolated on a filter. The solid was then allowed to dry overnight under a nitrogen atmosphere before being isolated (548.6 mg). While the specific formulation of the solid is uncertain, it is presumed to be the U(IV) hydrate, $U(SO_4)_2(H_2O)_x$. A species of known hydration was obtained by dissolving 200 mg of $U(SO_4)_2(H_2O)_x$ in 500 μL of 1.0 M H_2SO_4, which resulted in the formation of green block crystals of $U(SO_4)_2(H_2O)_7{\cdot}2H_2O$ (**1**) (70.0 mg) and the concomitant deposition an unidentified green microcrystalline solid over the course of several days. (It should be noted that isolation of **1** appears to be highly sensitive to crystallization conditions and frequently results in the deposition of the unidentified microcrystalline material as the sole product.) Additionally, isolated crystals of **1** quickly (<20 min) form a pale patina on the surface even when stored under nitrogen possibly due to desolvation) IR (KBr pellet, cm^{-1}): 3965(sh, w), 3516(sh, s), 3344(s), 3178(s), 2828(sh, m), 2334(w), 2126(sh, w), 2031(w), 1964(w), 1637(m), 1212(sh, s), 1165(sh, s), 1119(vs), 1088(vs), 1043(vs), 1005(sh, s), 996(s, ν_1), 675(sh, m), 649(sh, m), 620(sh, m), 602(s), 440(m). Raman (cm^{-1}): 3821, 3280, 2441, 1703, 1497, 1144 (ν_3), 1051(sh) (ν_3), 1042 (ν_3), 1006 (ν_1), 620 (ν_4), 599 (ν_4), 460(sh) (ν_2), 440 (ν_2), 389, 278, 256(sh), 229(sh), 174(sh), 159, 125.

$U(SO_4)_2(H_2O)_4{\cdot}H_2O$ (2). On one occasion, a few irregularly shaped green crystals were present in the crystallization of **1**. Characterization of one of these crystals by X-ray diffractometry revealed the presence of the penta-hydrate species, $U(SO_4)_2(H_2O)_4{\cdot}H_2O$ (**2**). Because of the serendipitous nature of this crystallization, further characterization **2** was not possible.

Synthesis for Compounds 3−5. In a 2 mL shell vial, 200 μL of 1.0 M H_2SO_4 (0.2 mmol) and 200 μL of 0.5 M M_2SO_4 (M = K, **3**; Rb, **4**; Cs, **5**) (0.1 mmol) were added to 10 mg (0.017 mmol) of crystalline $U(SO_4)_2(H_2O)_7{\cdot}xH_2O$ (**1**) resulting in dissolution of the crystals and the formation of a light green solution. The solutions were stored uncapped in an N_2 atmosphere for several days resulting in the deposition of crystalline material as described below.

$[K_8][U_2(SO_4)_8]{\cdot}6H_2O$ (3). $[K_8][U_2(SO_4)_8]{\cdot}6H_2O$ (**3**) was isolated as green block crystals (13.0 mg, 92% yield). IR (KBr pellet, cm^{-1}): 4401(w), 4257(w), 4044(w), 3601(w), 3478(m), 3293(w), 3061(w),

dx.doi.org/10.1021/ic301291w | Inorg. Chem. 2012, 51, 9481−9490

Table 2. Selected Bond Lengths and Interactions (Å) for Complexes 1−5

1		2		3		4		5	
U1−O1	2.337(3)	U1−O1	2.328(5)	U1−O1	2.424(3)	U1−O1	2.418(4)	U1−O1	2.247(6)
U1−O5	2.443(4)	U1−O2*	2.317(5)	U1−O2	2.420(3)	U1−O2	2.390(4)	U1−O5	2.453(7)
U1−O6	2.454(4)	U1−O5	2.372(7)	U1−O5	2.407(3)	U1−O5	2.432(4)	U1−O6	2.417(7)
U1−O7	2.434(3)	U1−O6	2.397(8)	U1−O6	2.433(3)	U1−O6	2.423(4)	U1−O7	2.362(6)
U1−O8	2.396(3)	U1−O7	2.392(5)	U1−O9	2.393(3)	U1−O9	2.399(4)	U1−O9	2.464(6)
U1−O9	2.456(4)	U1···O8	2.865(11)	U1−O10	2.380(3)	U1−O10	2.387(4)	U1−O10	2.504(6)
S1−O1	1.489(3)	U1···O8*	2.777(11)	U1−O13	2.477(3)	U1−O13	2.450(4)	U1−O11	2.391(6)
S1−O2	1.469(3)	S1−O1	1.487(5)	U1−O14	2.463(3)	U1−O14	2.491(4)	U1−O13	2.425(7)
S1−O3	1.469(3)	S1−O2	1.498(5)	U1−O15	2.343(3)	U1−O15	2.346(4)	U1−O14	2.460(6)
S1−O4	1.475(3)	S1−O3	1.459(5)	S1−O1	1.522(3)	S1−O1	1.515(4)	S1−O1	1.502(7)
O2···O8*	2.704(4)	S1−O4	1.459(6)	S1−O2	1.507(3)	S1−O2	1.529(4)	S1−O2	1.453(7)
O2···O9*	2.735(4)			S1−O3	1.457(3)	S1−O3	1.433(5)	S1−O3	1.451(7)
O3···O7*	2.746(4)			S1−O4	1.452(3)	S1−O4	1.459(5)	S1−O4	1.463(7)
O3···O7*	2.776(4)			S2−O5	1.516(3)	S2−O5	1.515(4)	S2−O5	1.490(7)
O4···O5*	2.739(4)			S2−O6	1.507(3)	S2−O6	1.508(4)	S2−O6	1.489(7)
O4···O6*	2.784(4)			S2−O7	1.455(3)	S2−O7	1.445(5)	S2−O7*	1.498(7)
O8···O10*	2.649(5)			S2−O8	1.449(3)	S2−O8	1.445(4)	S2−O8	1.432(7)
				S3−O9	1.512(3)	S3−O9	1.504(4)	S3−O9	1.493(7)
				S3−O10	1.521(3)	S3−O10	1.513(5)	S3−O10	1.488(7)
				S3−O11	1.454(3)	S3−O11	1.455(4)	S3−O11*	1.470(7)
				S3−O12	1.452(3)	S3−O12	1.444(5)	S3−O12	1.429(7)
				S4−O13	1.497(3)	S4−O13	1.496(4)		
				S4−O14	1.491(3)	S4−O14	1.486(4)		
				S4−O15*	1.495(3)	S4−O15*	1.486(4)		
				S4−O16	1.442(3)	S4−O16	1.437(5)		

2938(w), 2922(m), 2861(w), 2852(w), 2494(w), 2372(w), 2222(w), 2172(w), 2124(w), 2094(w), 2008(w), 1961(w), 1895(w), 1635(m), 1607(m), 1423(sh, m), 1257(vs), 1229(vs), 1195(m), 1150(vs), 1143(vs), 1076(vs), 1056(vs), 992(s), 980(s, ν_1), 950(vs, ν_1), 674(m), 654(sh, vs), 653(vs), 639(vs), 623(m), 618(sh, s), 614(s), 596(s), 594(sh), 530(m), 499(m), 425(w). Raman (cm^{-1}): 2920, 1261, 1235, 1180, 1149, 1142, 1044, 985 (ν_1), 962 (ν_1), 947(sh), 678, 658, 647, 636, 626, 614, 609, 604(sh), 527, 505(sh), 498, 420, 240, 170(sh), 143, 130(sh).

$[Rb_8][U_2(SO_4)_8]\cdot 2.5H_2O$ (4). $[Rb_8][U_2(SO_4)_8]\cdot 2.5H_2O$ (**4**) was isolated as green block crystals (9.6 mg, 58% yield). IR (KBr pellet, cm^{-1}): 4391(w), 4257(w), 4049(w), 3914(w), 3611(m), 3487(w), 3463(m), 3225(w), 3061(w), 2817(w), 2460(w), 2344(w), 2200(w), 2159(w), 2112(w), 2070(w), 1996(w), 1931(w), 1898(w), 1610(w), 1605(w), 1399(w), 1264(sh, vs), 1253(vs), 1244(sh, vs), 1225(vs), 1194(s), 1148(vs), 1140(vs), 1084(vs), 1054(vs), 991(vs), 981(s, ν_1), 952(vs, ν_1), 942(s), 672(m), 652(vs), 649(vs), 640(vs), 622(s), 617(sh, s), 613(s), 596(s), 592(sh, s), 524(w), 497(m), 423(w), 418(w). Raman (cm^{-1}): 3531, 2465, 1753, 1637, 1254, 1231, 1180, 1147, 1137, 1047, 984 (ν_1), 961 (ν_1), 946, 676, 656, 647, 638, 624, 612, 601, 596, 524, 501, 494, 424(sh), 419, 235, 224(sh), 212(sh), 177(sh), 166, 142(sh), 132.

$[Cs_2][U(SO_4)_3(H_2O)_2]$ (5). $[Cs_2][U(SO_4)_3(H_2O)_2]$ (**5**) was isolated as clusters of crystalline green needles cocrystallizing with an unidentified minor species present in the form of light green/teal plates. IR (KBr pellet, cm^{-1}): 4123(w), 3357(sh, w), 3210(w), 3081(w), 2334(w), 2311(w), 2205(w), 2144(w), 1997(w), 1923(w), 1616(w), 1552(w), 1252(s), 1197(s), 1169(s), 1164(s), 1149(s), 1132(sh, s), 1089(s), 1054(vs), 1041(sh, vs), 1034(vs), 986(s, ν_1), 975(s, ν_1), 950(sh, m), 833(w), 796(w), 649(s), 640(s), 612(s), 601(m), 593(sh, m), 496(w), 455(w), 443(w). Raman (cm^{-1}): 2457, 1750, 1256, 1203, 1146, 1072, 1056, 1042, 991 (ν_1), 981 (ν_1), 648, 646(sh), 642, 641(sh), 636, 633, 629(sh), 622(sh), 615, 610, 607, 588, 509, 505(sh), 503(sh), 500(sh), 497, 448, 418, 412, 388, 325, 281, 241, 213(sh), 188, 171, 148, 140, 131.

Vibrational Spectroscopy. IR samples were diluted (~2−5 wt %) with dry KBr and pressed into a pellet before being collected on a Nicolet Nexus 870 FTIR system. Data were collected using 16 scans over 4000−400 cm^{-1} with a resolution of 2 cm^{-1}. Raman data were collected on randomly oriented single crystals using a Renishaw inVia Raman microscope with a circularly polarized excitation line of 532 nm.

X-ray Crystallography. The solid state molecular structures for complexes **1**−**5** were determined similarly with exceptions noted. Crystals were mounted on a glass fiber under Paratone-N oil. Full spheres of data (0.5° frame widths) were collected using a Bruker SMART diffractometer equipped with an APEXII detector using Mo Kα radiation. All data were collected at 100 K using an Oxford Cryosystems cryostat. The data were integrated and corrected for absorption using the APEX2 suite of crystallographic software, while structure solutions and refinements were completed using XShell.[30] Compound **1** was solved and refined as a twin using CELL_NOW and twinabs with the two components resolved in a 91:9 ratio. The constraints SIMU and DELU were applied during refinement of the anisotropic thermal parameters for the oxygen atoms in compound **5**. Metrical data for the structure solutions and refinements are available in Tables 1 and 2.

RESULTS

Structure Descriptions. The solid state molecular structures of compounds **1**−**5** each contain one or more sulfate ligands bound to a U(IV) metal center. While 18 binding modes have been crystallographically characterized for the sulfate ligand,[9] only 4 distinct modes are represented in the complexes reported here; monodentate, bidentate-chelating, bidentate-bridging, and tridentate-bridging (Figure 1). In the tridentate-bridging binding mode, the sulfate chelates one metal center in a bidentate fashion and binds to the second metal though a monodentate interaction to produce a bridge between the two metals. This binding mode has been previously observed in An(IV) sulfate complexes such as $Cs_2Th(SO_4)_3(H_2O)_2$,[21] $Cs_2Np(SO_4)_3(H_2O)\cdot H_2O$,[26] $K_8Pu_2(SO_4)_8\cdot 5H_2O$,[15] and $Rb_8Pu_2(SO_4)_8\cdot 4H_2O$.[15]

dx.doi.org/10.1021/ic301291w | Inorg. Chem. 2012, 51, 9481−9490

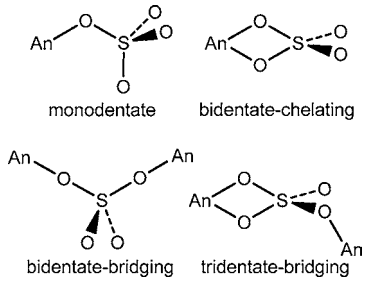

Figure 1. Graphical depiction of the four sulfate binding modes present in complexes **1**–**5**.

The neutral U(IV) sulfate $U(SO_4)_2(H_2O)_7{\cdot}2H_2O$ (**1**) is isostructural to the previously reported thorium analogue[16,22] and crystallizes as green blocks in the monoclinic space group $P2_1/m$ (Figure 2). The molecular complex consists of a

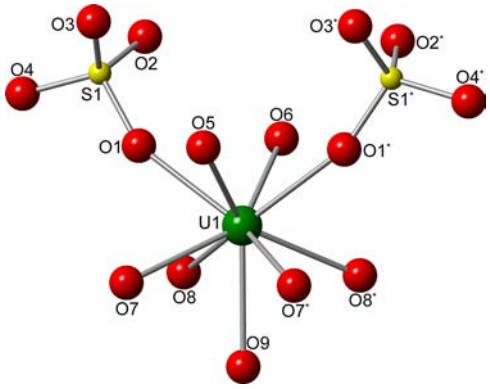

Figure 2. Ball and stick model of $U(SO_4)_2(H_2O)_7{\cdot}2H_2O$ (**1**) depicting the connectivity around the metal center.

uranium atom bound by two monodentate sulfate ligands and seven water molecules, resulting in a 9-coordinate complex with monocapped square antiprismatic geometry.[22] To our knowledge, complex **1** is only the second structurally characterized U(IV) compound containing a monodentate terminal sulfate and the U–OSO_3 distance (2.337(3) Å) is consistent with the monodentate sulfate ligands in $Na_{1.5}(NH_4)_{4.5}[U(SO_4)_5(H_2O)]{\cdot}H_2O$ (2.295(5) Å and 2.325(5) Å).[13] The U–O bond length of the coordinated water molecules range from 2.396(3) to 2.456(4) Å and are also consistent with previously reported U(IV) aquo complexes.[31–33] Similar to what was observed in the thorium analogue,[16,22] complex **1** contains hydrogen bonding interactions between the unbound sulfate oxygens and bound waters on neighboring molecules in the crystal structure (Figure 3). These O···O distances range from 2.704(4) to 2.784(4) Å and agree with literature values for previously identified hydrogen bonding interactions.[34–36] Additional hydrogen bonding is also observed between one of the bound waters (O8) and the free water molecule (O10) located within the crystal structure (2.649(5) Å).

On one occasion, we analyzed a single crystal from the synthesis of **1** and characterized it as the neutral complex $U(SO_4)_2(H_2O)_4{\cdot}H_2O$ (**2**), a new hydration state of the β-phase previously reported by Kierkegaard (Figure 4).[29] Complex **2** crystallizes in the orthorhombic space group *Pnma* and consists of two-dimensional extended sheets formed through bidentate-bridging sulfate ligands (Figure 5). Each metal center has an eight-coordinate square antiprismatic geometry[37] with the

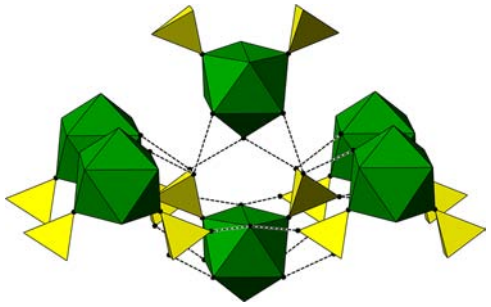

Figure 3. A polyhedral representation depicting the hydrogen bonding in $U(SO_4)_2(H_2O)_7{\cdot}2H_2O$ (**1**) (U = green, sulfate = yellow, black = oxygen).

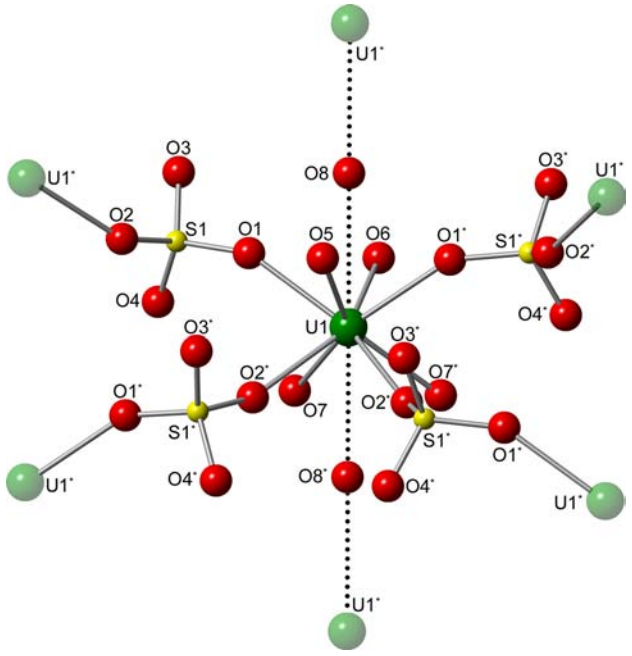

Figure 4. Ball and stick model of $U(SO_4)_2(H_2O)_4{\cdot}H_2O$ (**2**) depicting the connectivity around the metal center and bridging to adjacent uranium atoms.

uranium bound by four bidentate-bridging sulfate ligands and four water molecules. The U–OH_2 bond distances for the bound water molecules in **2**, 2.372(7) to 2.397(8) Å, are comparable to the shortest U–OH_2 bond in **1**, 2.396(3) Å. Similarly, the U–OSO_3 bonds for complexes **1** (2.337(3) Å) and **2** (2.317(5) and 2.328(5) Å) correlate well with each other.

The primary feature of complex **2** that distinguishes it from Kierkegaard's β-phase is a fifth water molecule in the crystal structure that is not present in the previously reported structure (Figure 4). This water is located within the two-dimensional sheets and sits directly between two uranium atoms with U···O distances of 2.777(11) and 2.865(11) Å and the U···O···U* angle of 179.4(4)° (Figure 5). These U···O distances are similar to the O···O distances observed for the hydrogen bonding in **1** and result in a pseudo 10-coordinate bicapped square antiprismatic geometry around the uranium. The differing hydration state between $U(SO_4)_2(H_2O)_4$ and **2** may be a result of the elevated temperature at which the previously reported complex was synthesized versus the ambient conditions employed in this study.[29]

dx.doi.org/10.1021/ic301291w | *Inorg. Chem.* 2012, 51, 9481–9490

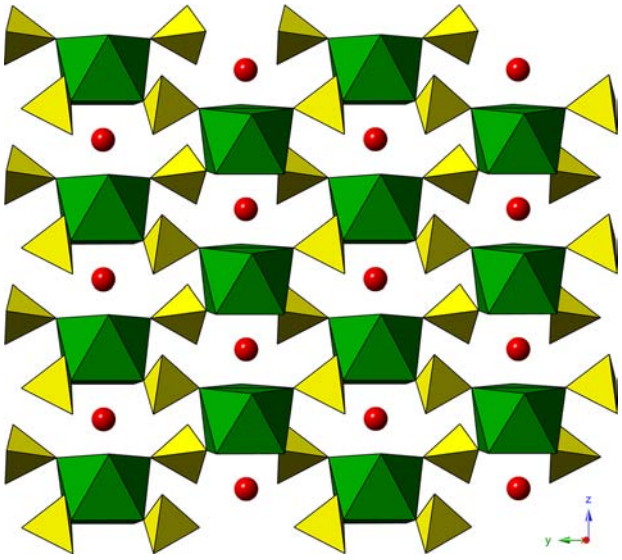

Figure 5. A polyhedral representation depicting the crystal packing of $U(SO_4)_2(H_2O)_4{\cdot}H_2O$ (**2**) (U = green, sulfate = yellow, water = red).

Crystallization of U(IV) sulfates from aqueous solutions of K_2SO_4 or Rb_2SO_4 results in the formation of $K_8U_2(SO_4)_8{\cdot}6H_2O$ (**3**) and $Rb_8U_2(SO_4)_8{\cdot}2.5H_2O$ (**4**), respectively (Figure 6). Complexes **3** and **4** are isostructural to both

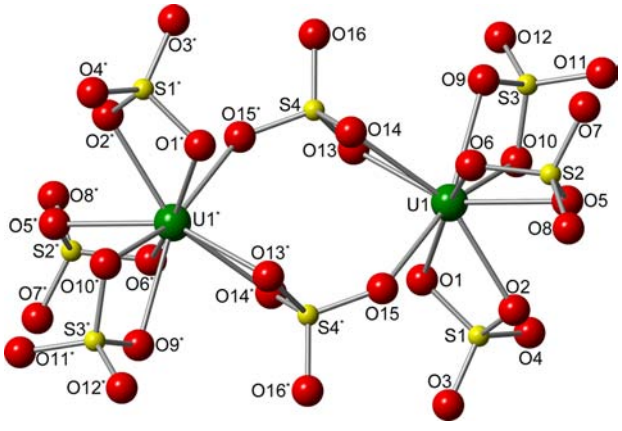

Figure 6. Ball and stick model of complexes $K_8U_2(SO_4)_8{\cdot}6H_2O$ (**3**) and $Rb_8U_2(SO_4)_8{\cdot}2.5H_2O$ (**4**) depicting the connectivity around the metal center.

each other and their plutonium analogues, $K_8Pu_2(SO_4)_8{\cdot}5H_2O$ and $Rb_8Pu_2(SO_4)_8{\cdot}4H_2O$,[15] all four of which crystallize in the monoclinic space group $P2_1/c$ and differ only by the number of unbound water molecules found in the crystal structure (Figure 7 and S4). Both compounds **3** and **4** contain molecular dimeric units comprised of two 9-coordinate uranium(IV) centers, where each metal is bound by three bidentate-chelating sulfate ligands and dimerized through two tridentate-bridging sulfates. The U−O bond lengths of the bidentate-chelating sulfate ligands range from 2.380(3) to 2.433(3) Å for complex **3** and 2.387(4) to 2.432(4) Å for complex **4**. For both complexes, the longer of these bonds are similar to the shortest U−O bonds for the chelating sulfates in $Na_{1.5}(NH_4)_{4.5}[U(SO_4)_5(H_2O)]{\cdot}H_2O$, which range from 2.424(5) to 2.491(5) Å.[13] The tridentate-bridging sulfate ligands of **3** exhibit a U−O distance of 2.343(3) Å for the monodentate bond, while the chelating bond lengths are 2.463(3) and 2.477(3) Å. The

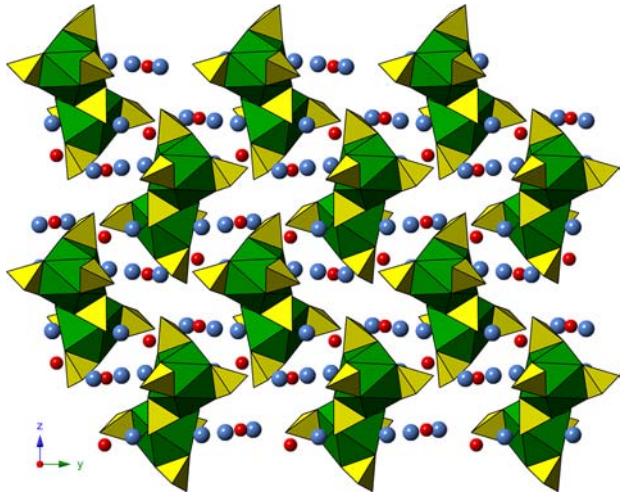

Figure 7. A polyhedral representation depicting the crystal packing of $Rb_8U_2(SO_4)_8{\cdot}2.5H_2O$ (**4**) (U = green, sulfate = yellow, water = red, Rb = blue).

corresponding bonds of complex **4** are statistically identical within the 3σ rule, measuring 3.346(4), 2.450(4), and 2.491(4) Å for the monodentate and chelating bonds, respectively.

Under the same conditions employed for the synthesis complexes **3** and **4**, the use of Cs_2SO_4 resulted in the formation of $Cs_2U(SO_4)_3(H_2O)_2$ (**5**) (Figure 8). Complex **5** crystallizes

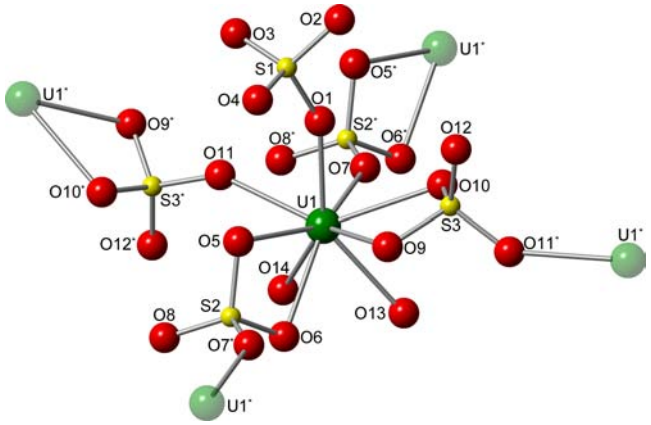

Figure 8. Ball and stick model of $Cs_2U(SO_4)_3(H_2O)_2$ (**5**) depicting the connectivity around the metal center and sulfate bridging to adjacent uranium atoms.

as green plates in the monoclinic space group $P2_1/c$. The U(IV) center is bound by one terminal monodentate sulfate and four tridentate-bridging sulfates that link the metal centers to form two-dimensional sheets (Figure 9). In addition to the sulfate ligands, the primary coordination sphere of the uranium contains two bound water molecules, resulting in a 9-coordinate metal center. The U−O bond length of the terminal monodentate sulfate in **5**, 2.247(6) Å, is the shortest reported uranium−sulfate bond for a U(IV) complex. This bond is 0.09 Å shorter than the U−O sulfate bond in the neutral parent complex (2.337(3) Å) and 0.05 Å less than the shortest uranium sulfate bond in $Na_{1.5}(NH_4)_{4.5}[U(SO_4)_5(H_2O)]{\cdot}H_2O$ (2.295(5) Å).[13] The U−O bonds of the tridentate-bridging sulfates in **5** are similar to those observed in complexes **3** and **4**, measuring 2.362(6) Å and 2.391(6) Å for the two monodentate bonds and ranging from 2.417(7) Å to 2.504(6) Å for the four

dx.doi.org/10.1021/ic301291w | Inorg. Chem. 2012, 51, 9481−9490

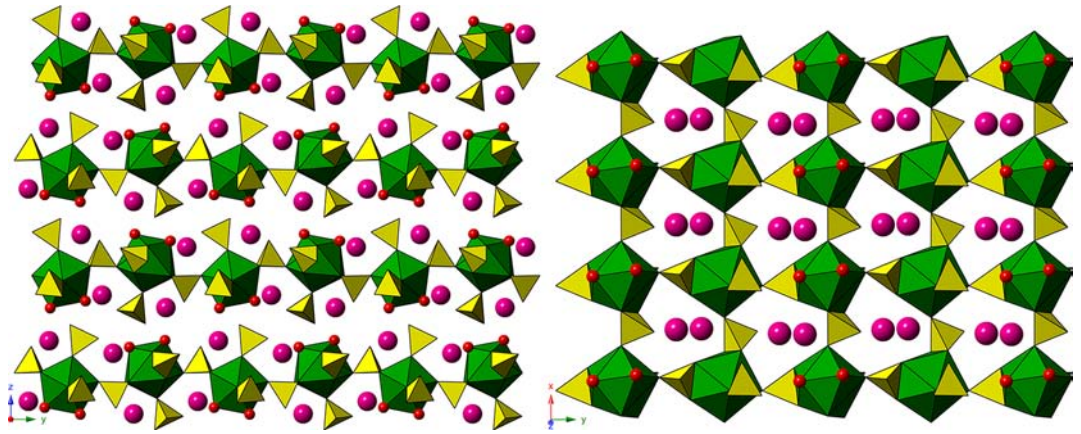

Figure 9. A polyhedral representation depicting the two-dimensional sheets found in $Cs_2U(SO_4)_3(H_2O)_2$ (**5**) as viewed down the *x* axis (left) and *z* axis (right) (U = green, sulfate = yellow, water = red, Cs = magenta).

chelating interactions. Finally, the two bound water molecules reside 2.425(7) Å and 2.460(6) Å from the metal center, which is consistent with the distances observed in complexes **1** and **2**.

The solid state molecular structures for compounds **1** and **3**−**5** have also been confirmed using powder diffractometry. The powder pattern and refinement for each complex are provided in the Supporting Information (Figures S22−S25).

Vibrational Spectroscopy. In addition to single crystal X-ray diffractometry, complexes **1** and **3**−**5** have been characterized by Raman and IR spectroscopy. The vibrational spectra for the complexes reported here are dominated by signals correlating to the sulfate anions, since the modes associated with the spherical U(IV) and alkali metal cations are predominantly IR and Raman silent rotational degrees of freedom.

For a penta-atomic molecule with tetrahedral symmetry (T_d) such as sulfate, four distinct bands are found in the Raman and IR spectra: the A_1 (ν_1 symmetric stretch) at 956−1064 cm^{-1}, the doubly degenerate E (ν_2 bending) at 407−527 cm^{-1}, and two triply degenerate T_2 modes (ν_3 asymmetric stretch) at 1031−1269 cm^{-1} and (ν_4 bending) 578−669 cm^{-1} (Table 3).[38]

Table 3. The Correlation between T_d and C_1 Symmetry and the Expected Ranges for the Corresponding Vibrations

T_d symmetry	C_1 symmetry	spectral region (cm^{-1})
A_1 (ν_1 symmetric stretch)	1 *A*	956−1064
E (ν_2 bending)	2 *A*	407−527
T_2 (ν_3 asymmetric stretch)	3 *A*	1031−1269
T_2 (ν_4 bending)	3 *A*	578−669

When the sulfate has T_d symmetry such as in an aqueous solution of Na_2SO_4, all four modes are Raman active and both the ν_3 and ν_4 modes are IR active, resulting in a prediction of four signals in the Raman spectrum and two in the IR.[38,39] As the symmetry of the sulfate is reduced, either by coordination to a metal cation or as a result of positioning within a crystal lattice, additional vibrational modes arise from the lifting of the degeneracy in the E and T_2 modes (Table 3). Inspection of the crystal structures and subsequent factor analysis demonstrates that the degeneracies of the E and T_2 modes are lifted in all of the complexes reported herein because, in all cases, the sulfate resides on the general position with C_1 symmetry. It should be noted that independent of the ion symmetry, the ν_1 symmetric stretch is consistently the most intense signal in the sulfate Raman spectrum with the other signals ranging from 3 to 50% of its relative intensity.[38]

As previously discussed, the solid state molecular structure of complex **1** contains a single crystallographically unique sulfate ligand bound in a monodentate fashion to the uranium atom. On the basis of the C_1 site symmetry of the sulfate within the crystal, group theory predicts a lifting of the degeneracy in the E and T_2 modes resulting in nine total ligand vibrational modes (one ν_1, two ν_2, three ν_3, and three ν_4,). We have assigned the intense signal at 1006 cm^{-1} in the Raman spectrum to the ν_1 symmetric stretching mode, with the corresponding signal in the IR spectrum occurring at 996 cm^{-1} (Figure 10). In addition

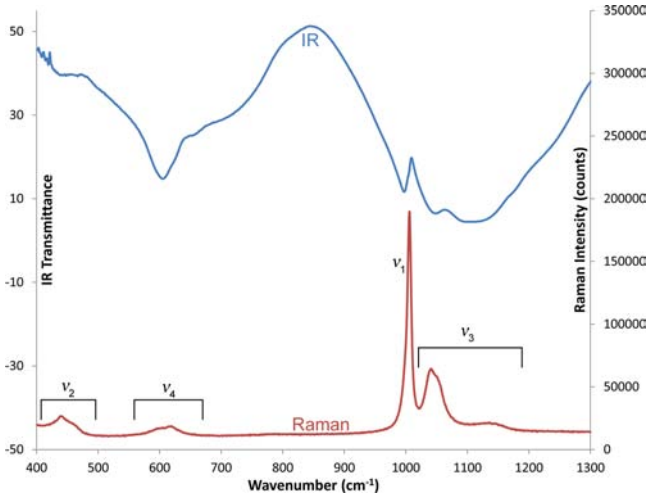

Figure 10. IR (blue) and Raman (red) spectra of $U(SO_4)_2(H_2O)_7{\cdot}2H_2O$ (**1**).

to the single ν_1 signal, we observed two ν_2 (460(sh) and 440 nm), three ν_3 (1144, 1051(sh), and 1042 nm), and two ν_4 signals (620 and 599 nm) for a total of eight Raman active vibrational modes (the third ν_4 mode may not be visible due to broadening or signal overlap). The IR spectrum for complex **1** also exhibits a band at 1637 cm^{-1} corresponding to water within the crystal structure. Both the Raman and IR spectra for complex **1** are consistent with the previously reported spectra for the isostructural thorium analogue.[22]

As is expected for isostructural complexes, both the Raman and IR spectra of **3** and **4** are very similar, particularly with

dx.doi.org/10.1021/ic301291w | *Inorg. Chem.* 2012, 51, 9481−9490

respect to the sulfate region (Figure 11). The solid state molecular structure for both complexes contains two sulfate

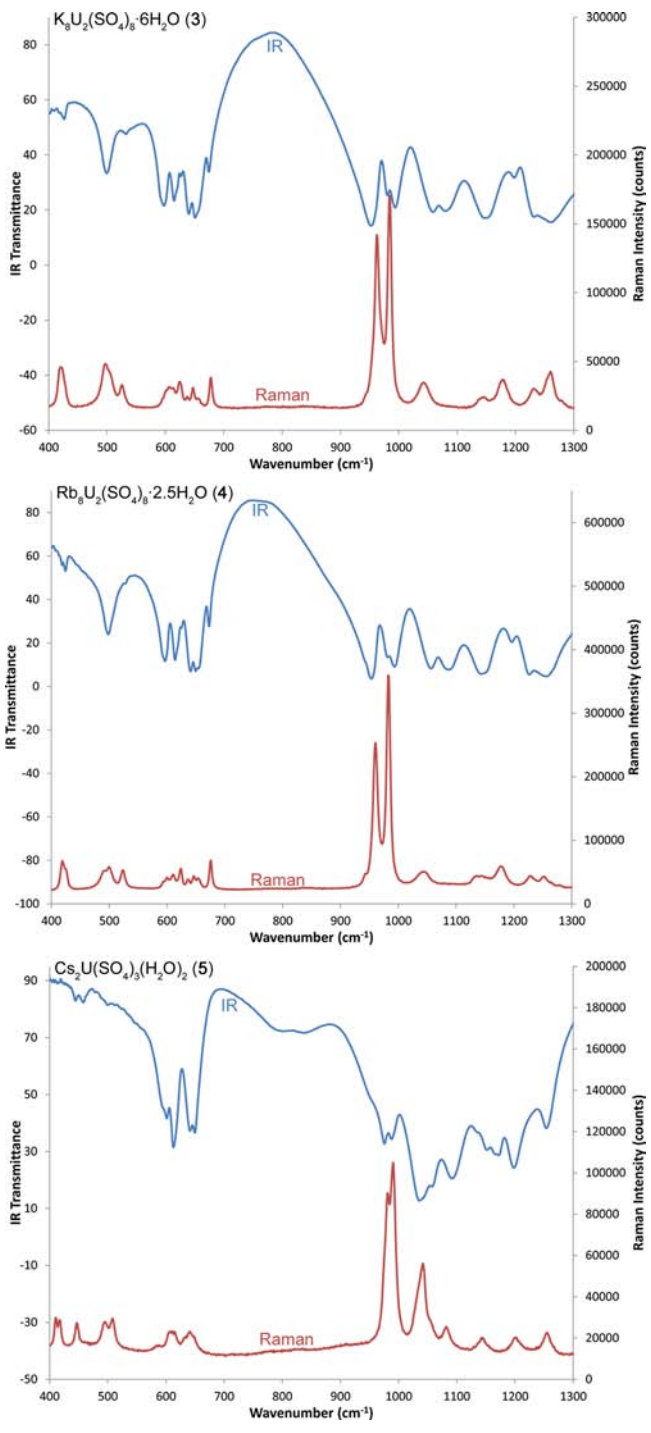

Figure 11. IR (blue) and Raman (red) spectra of $K_8U_2(SO_4)_8{\cdot}6H_2O$ (**3**) (top), $Rb_8U_2(SO_4)_8{\cdot}2.5H_2O$ (**4**) (middle), and $Cs_2U(SO_4)_3(H_2O)_2$ (**5**) (bottom).

binding modes, bidentate-chelating and tridentate-bridging, among the four crystallographically unique sulfate tetrahedra. Similar to complex **1**, all of the sulfates in **3** and **4** reside on general positions of C_1 symmetry within the crystal, resulting in the degeneracy on the E and T_2 modes being lifted. The presence of multiple sulfate binding modes is manifested by two separate intense signals in the ν_1 region of the Raman spectrum for complexes **3** (962 and 985 cm^{-1}) and **4** (961 and 984 cm^{-1}). As predicted by group theory and factor analysis, the corresponding ν_1 vibrations are also observed in the IR spectrum where they appear at 950 and 980 cm^{-1} for **3** and 952 and 981 cm^{-1} for **4**. The Raman spectra for both complexes **3** and **4** exhibit an additional minor signal within the ν_1 region (947 cm^{-1}, **3**; 946 cm^{-1}, **4**) that may be attributed to chemical inequivalence of the bidentate-chelating sulfate ligands within the molecule.

In addition to the observed ν_1 signals, group theory predicts that complexes **3** and **4** will exhibit two ν_2, three ν_3, and three ν_4 signals in both the Raman and IR spectrum for each unique sulfate ligand. The Raman spectrum of **3** contains four signals within the ν_2 region, six signals within the ν_3 region, and eight signals within the ν_4 region, while the corresponding regions of the IR spectrum display three, seven, and nine bands, respectively. The Raman and IR spectra for **4** are very similar to those of **3**, only varying in the number of bands observed in the ν_2 region of the Raman (five signals), and the ν_2 (four signals) and ν_3 (nine signals) regions of the IR. As with the ν_1 region, the additional signals observed in the ν_2, ν_3, and ν_4 regions of both complexes could be attributed to chemical inequivalence of the multiple bidentate-chelating sulfate ligands within each complex. In addition to the sulfate vibrations, the IR spectra of **3** and **4** also contain bands located at 1607 and 1635 cm^{-1} for **3** and 1605 and 1610 cm^{-1} for **4** consistent with the presence of water within the solid state molecular structure.

The Raman spectrum for complex **5** contains two intense vibrations in the ν_1 band at 991 and 981 cm^{-1} with corresponding bands in the IR at 986 and 975 cm^{-1}. Although the solid state structure contains three crystallographically unique sulfates, the presence of only two ν_1 signals indicates that the ligands may have similar chemical environments, resulting in an overlapping of the bands. As with the other complexes reported here, the sulfate ligands for complex **5** are lowered in symmetry due to their position in the crystal lattice, resulting in the lifting of the degeneracy on the E and T_2 vibrational modes. This results in the presence of 8 signals within the ν_2 region, 6 signals within the ν_3 region, and 12 signals within the ν_4 region of the Raman spectrum, while the corresponding regions of the IR spectrum displaying 2, 10, and 5 bands, respectively. For complex **5**, the water bands, located at 1552 and 1616 cm^{-1} in the IR spectrum, show significant broadening and shifting in comparison to the previously discussed complexes.

DISCUSSION

Herein, the reported compounds exhibit a variety of structural conformations including monomeric and dimeric arrangements as well as two-dimensional extended solids. Unlike the mononuclear ligands such as oxygen and halogens used by Seaborg to elucidate initial trends in the actinides, the diversity of coordination modes available to sulfate makes it more difficult to directly correlate the structural properties of these complexes to the intrinsic chemistry of the metal ion. However, characterization of the complexes presented here has helped to identify the emergence of structural trends within this class of compounds across the An(IV) series and emphasizes that the chapter on the crystal chemistry of the An(IV) sulfates is far from complete.

With the addition of this work, there appear to be three primary phases of the neutral An(IV) sulfate complexes with the formula $An(SO_4)_2(H_2O)_x$ that occur within the actinides:

dx.doi.org/10.1021/ic301291w | Inorg. Chem. 2012, 51, 9481−9490

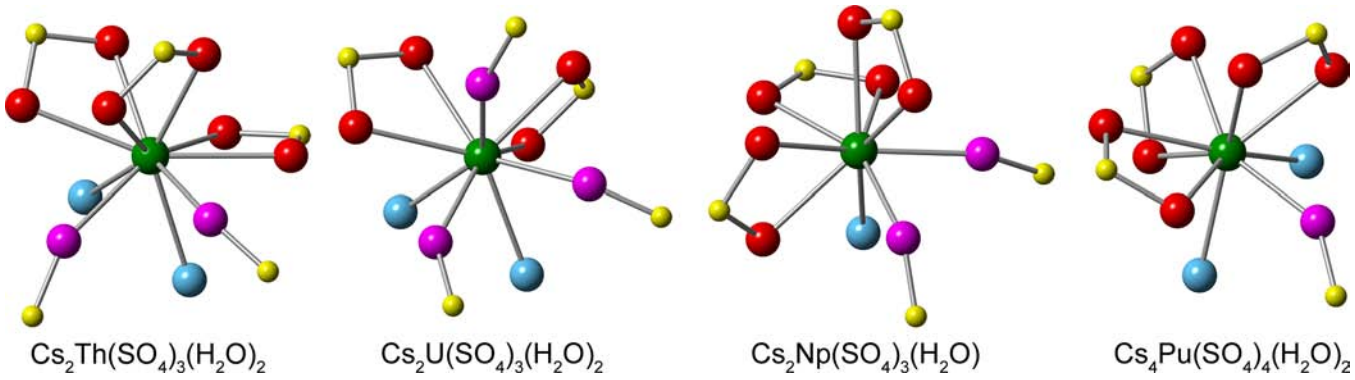

Figure 12. Ball and stick model depicting the primary coordination sphere of the metal in the Cs stabilized An(IV) sulfate series (An = green, S = yellow, oxygen in bidentate interaction = red, oxygen in monodentate interaction = magenta, water = blue).

β-$An(SO_4)_2(H_2O)_4$ (An = U,[29] Np,[27] Pu[28]), $An(SO_4)_2(H_2O)_7{\cdot}2H_2O$ (An = Th,[16,22] U), and $An(SO_4)_2$ (An = Th, U).[18] The actinide cations in these compounds are bound by between two and eight sulfate ligands and can contain from zero to seven water molecules in the primary coordination sphere. This variety of neutral An(IV) sulfates with the formula $An(SO_4)_2(H_2O)_x$ makes it difficult to elucidate periodic trends across the actinide series since the structural variations most likely arise from a combination of differences in the conditions under which these compounds were synthesized. Our analysis aims at comparing complexes synthesized under similar conditions, as their variations should arise more directly from inherent differences between the metal centers.

In addition to $U(SO_4)_2(H_2O)_7{\cdot}2H_2O$ (**1**), only three other structurally characterized neutral An(IV) sulfates that have been synthesized at room temperature: $Th(SO_4)_2(H_2O)_7{\cdot}2H_2O$,[16,22] $Th(SO_4)_2(H_2O)_6{\cdot}2H_2O$,[19] and α-$Pu(SO_4)_2(H_2O)_4$.[15] This set of four compounds is unique because it contains only the second U(IV), Np(IV), or Pu(IV) sulfate complex that is isostructural to a thorium analogue, $Th(SO_4)_2(H_2O)_7{\cdot}2H_2O$ and $U(SO_4)_2(H_2O)_7{\cdot}2H_2O$. Both of these compounds are synthesized through mild reactions and crystallize under similar conditions. The only other instance where a pair of isostructural An(IV) sulfate compounds includes a thorium species is $An(SO_4)_2$ (An = Th, U).[18] In this case, the metal center is bound by eight tetradentate-bridging sulfate ligands forming a three-dimensional extended lattice. This compound is formed using aggressive conditions (100% H_2SO_4 and thermolysis at 300 °C), which help to exclude water from the primary coordination sphere of the metal and allow complexation of eight sulfate ligands. The elevated temperature and lack of water in this synthesis makes it difficult to extrapolate these results to the complexes reported here since they are synthesized under much milder conditions.

In addition to **1**, we also characterized a second neutral U(IV) sulfate species, $U(SO_4)_2(H_2O)_4{\cdot}H_2O$ (**2**), which is a new hydration state of the known β-phase. In a previously reported synthesis of the neutral U(IV) sulfate tetrahydrate, Kierkegaard describes heating the reaction at 90 °C for a week to allow for isolation of $U(SO_4)_2(H_2O)_4$, the β-$An(IV)(SO_4)_2(H_2O)_4$ phase common to Ce(IV),[40] U(IV),[29] Np(IV),[27] and Pu(IV).[28] In contrast to the elevated temperatures reported by Kierkegaard, we isolated the single crystal of complex **2** from a crystallization of **1** that had been sitting at room temperature for over a month. This result suggests that $U(SO_4)_2(H_2O)_7{\cdot}2H_2O$ (**1**) may lose water over time at room temperature, resulting in the formation of $U(SO_4)_2(H_2O)_4{\cdot}H_2O$ (**2**). Previously, thermogravimetric analysis of U(IV) neutral sulfate complexes performed by Golovnya and Bolotova in 1961 demonstrated that higher hydrates such as $U(SO_4)_2(H_2O)_8$ may lose up to four equivalents of water at 70 °C, resulting in the formation of $U(SO_4)_2(H_2O)_4$, which does not show further dehydration until 170 °C.[41]

As previously noted, the U(IV) and Pu(IV)[15] sulfate complexes containing potassium or rubidium cations ($K_8U_2(SO_4)_8{\cdot}6H_2O$ (**3**), $Rb_8U_2(SO_4)_8{\cdot}2.5H_2O$ (**4**), $K_8Pu_2(SO_4)_8{\cdot}5H_2O$, $Rb_8Pu_2(SO_4)_8{\cdot}4H_2O$) are all isostructural and vary only by the hydration state of the structure. In all four of these complexes, the actinide ion is bound by three bidentate-chelating and two tridentate-bridging sulfates to form discrete dimers where each metal center is 9-coordinate.

When attempting to compare the U and Pu species to other structurally characterized An(IV) sulfate analogues containing K^+ or Rb^+ cations, we find only two complexes containing potassium and no rubidium containing compounds. The first analogue is the thorium species $K_4Th(SO_4)_4(H_2O)_2$,[17] which exhibits a ligand arrangement significantly different to that observed for U and Pu. The thorium complex contains a 9-coordinate metal center bound by one monodentate, one bidentate-chelating, and four bidentate-bridging sulfates, as well as two water molecules that fill out the primary coordination sphere of the metal. Unlike the U and Pu species which both form discrete dimers, the Th complex crystallizes as one-dimensional chains where the metal atoms are connected through the bidentate-bridging sulfates.

The second, and more recently reported, An(IV) sulfate complex containing a potassium cation is the neptunium species $K_{5.5}(H_5O_2)_{0.5}Np(SO_4)_5$.[24] This complex crystallizes as monomeric units, each containing a 10-coordinate metal center bound by five bidentate-chelating sulfate ligands. Because of its crystallization at 150 °C and the presence of the dioxonium cation, it is difficult to compare the neptunium complex to the Th, U, and Pu analogues, which are all prepared at room temperature and charge balanced solely by potassium. The use of elevated temperatures in the Np(IV) synthesis could be responsible for the deviations in the chemical composition, coordination number, and binding modes observed when comparing it to the analogues formed by the bracketing elements in the actinide series.

The most complete and potentially most informative series of An(IV) sulfate complexes are those stabilized by Cs cations. The entire series from thorium through plutonium (with the exception of protactinium) has been structurally characterized

dx.doi.org/10.1021/ic301291w | Inorg. Chem. 2012, 51, 9481−9490

and all four of these species were synthesized at ambient temperature under similar conditions allowing for a direct comparison of the solid state structures (Figure 12). In the thorium complex, $Cs_2Th(SO_4)_3(H_2O)_2$, the metal center is bound by one terminal bidentate-chelating sulfate, four tridentate-bridging sulfates and two waters to form a 10-coordinate species.[21] Upon moving across the actinides to uranium, only a slight conformational change is required to form **5**, $Cs_2U(SO_4)_3(H_2O)_2$, which is isostructural to the thorium analogue except for the terminal sulfate is now monodentate resulting in a 9-coordinate metal center. The neptunium species[26] is polymorphic to both the Th and U analogues, but the ligand arrangement around the metal center exhibits minor differences. The terminal sulfate in $Cs_2Np(SO_4)_3(H_2O)\cdot H_2O$ is once again bidentate-chelating to the metal similar to the Th species, but now one of the water molecules resides unbound in the crystal structure resulting in a 9-coordinate metal center as was observed for the uranium complex. Interestingly, a significant change in both chemical composition and ligand arrangement is observed when continuing to traverse along the actinides to plutonium. The chemical formula for the plutonium analogue $Cs_4Pu(SO_4)_4(H_2O)_2$ contains an additional sulfate ligand as well as the two additional cesium atoms required for charge balancing. In the solid state, the plutonium species contains two crystallographically distinct environments, each containing a 9-coordinate metal center bound by one monodentate and three bidentate-chelating sulfate ligands, as well as two water molecules that fill out the primary coordination sphere. Interestingly, the plutonium complex forms discrete monomeric units, whereas the Th−Np complexes all crystallize as two-dimensional sheets with the metals connected by the tridentate-bridging sulfate ligands.

Examining changes in the ligand coordination within the Cs An(IV) sulfate series allows us to speculate about the underlying chemistry that may be responsible (Figure 12). A comparison of the sulfate binding modes for compounds within the Cs series reveals that the ratio of monodentate to bidentate interactions at the An(IV) center is 2:3, 3:2, 2:3, and 1:3 for the Th, U, Np, and Pu compounds, respectively. When traversing the series from thorium to uranium, the binding mode of the terminal sulfate ligand switches from bidentate to monodentate and the coordination number of the metal center is reduced from 10 to 9. This change in the coordination mode could be due to increased steric pressure resulting from the contraction of the ionic radius going from Th to U. Continuing across the series from uranium to neptunium, the transition of the terminal sulfate ligand from monodentate back to bidentate is accompanied by a loss of water and may be an effect of the greater Lewis acidity of the later An(IV) ions.[10,15,22] As previously mentioned, moving across the series from neptunium to plutonium results in the transition from two-dimensional sheets to discrete monomeric units. The presence of monomeric units in the plutonium complex is potentially due to the binding of a fourth sulfate ligand in solution before crystallization. The binding of four unique sulfate ligands in solution lowers the symmetry of the complex about the metal center and disrupts the formation of the extended network.

The overall trend extrapolated from the Cs An(IV) sulfate series may indicate that an increase in the Lewis acidity at the metal center promotes bidentate binding of the sulfate ligand as long as the complexation can outcompete the resulting increase in steric pressure associated with the actinide contraction. This hypothesis correlates well with the experimental results reported for the solution phase speciation in An(IV) sulfate systems that show a trend in the binding mode of sulfate from monodentate to bidentate when moving across the actinides from thorium to plutonium.[10,12−14]

CONCLUSION

In this work, we report the synthesis and characterization of four new U(IV) sulfate species, as well as the solid state molecular structure of $U(SO_4)_2(H_2O)_4\cdot H_2O$. These five compounds significantly increase the number of structurally characterized U(IV) sulfate complexes and provide valuable information to help investigate solid state periodic trends across the actinides. They also demonstrate the complexity of the An(IV) sulfate system and highlight the structural dependence on both synthetic conditions and the identity of the cation. Further study of both the solid and solution states of the An(IV) sulfates is important and could help elucidate structure and bonding trends across the actinide series in more complex ligand systems contributing to our development of a predictive framework for actinide coordination chemistry.

ASSOCIATED CONTENT

Supporting Information

Figures of the solid state molecular structures with ADP ellipsoids, crystallographic information in CIF format, IR (400−4900 cm^{-1}) spectra, Raman spectra (100−4100 cm^{-1}), and X-ray powder diffraction data for the reported complexes are available free of charge via the Internet at http://pubs.acs.org.

AUTHOR INFORMATION

Corresponding Author

*E-mail: rewilson@anl.gov.

Notes

The authors declare no competing financial interest.

ACKNOWLEDGMENTS

This work was performed at Argonne National Laboratory, operated for the United States Department of Energy, Office of Science, Office of Chemical Sciences, by UChicagoArgonne LLC under contract number DE-AC02-06CH11367.

REFERENCES

(1) Seaborg, G. T. *Chem. Eng. News* **1945**, *23*, 2190−2193.
(2) Seaborg, G. T. *Science* **1946**, *104* (2704), 379−386.
(3) Seaborg, G. T. Paper 21.1: Electronic Structure of the Heaviest Elements. In *The Transuranium Elements: Research Papers*; McGraw-Hill Book Co. Inc.: New York, 1949; Vol. 2.
(4) Diamond, R. M.; Street, K.; Seaborg, G. T. *J. Am. Chem. Soc.* **1954**, *76* (6), 1461−1469.
(5) Grenthe, I.; Fuger, J.; Konings, R. J. M.; Lemire, R. J.; Muller, A. B.; Cregu, C. N.-T.; Wanner, H. *Chemical Thermodynamics of Uranium*; OECD Publishing: Paris, 2004.
(6) Guillaumont, R.; Fanghänel, T.; Fuger, J.; Grenthe, I.; Neck, V.; Palmer, D. A.; Rand, M. H., *Update on the Chemical Thermodynamics of Uranium, Neptunium, Plutonium, Americiam, and Technetium*; Elsevier: Amsterdam, 2003.
(7) Lemire, R. J.; Fuger, J.; Nitsche, H.; Potter, P.; Rand, M. H.; Rydberg, J.; Spahiu, K.; Sullivan, J. C.; Ullman, W. J.; Vitorge, P.; Wanner, H. *Chemical Thermodynamics of Neptunium and Plutonium*; Elsevier: Amsterdam, 2001.
(8) Rand, M. H.; Fuger, J.; Grenthe, I.; Neck, V.; Rai, D. *Chemical Thermodynamics of Thorium*; OECD Publishing: Paris, 2008.

(9) Papatriantafyllopoulou, C.; Manessi-Zoupa, E.; Escuer, A.; Perlepes, S. P. *Inorg. Chim. Acta* **2009**, *362* (3), 634−650.
(10) Wilson, R. E. Structural Periodicity in Aqueous Pu(IV) Sulfates. *Inorg. Chem.* **2012**, *51* (16), 8942−8947.
(11) Dobler, M.; Guilbaud, P.; Dedieu, A.; Wipff, G. *New J. Chem.* **2001**, *25* (11), 1458−1465.
(12) Hennig, C.; Ikeda-Ohno, A.; Tsushima, S.; Scheinost, A. C. *Inorg. Chem.* **2009**, *48* (12), 5350−5360.
(13) Hennig, C.; Kraus, W.; Emmerling, F.; Ikeda, A.; Scheinost, A. C. *Inorg. Chem.* **2008**, *47* (5), 1634−1638.
(14) Hennig, C.; Schmeide, K.; Brendler, V.; Moll, H.; Tsushima, S.; Scheinost, A. C. *Inorg. Chem.* **2007**, *46* (15), 5882−5892.
(15) Wilson, R. E. *Inorg. Chem.* **2011**, *50* (12), 5663−5670.
(16) Albrecht, A. J.; Sigmon, G. E.; Moore-Shay, L.; Wei, R.; Dawes, C.; Szymanowski, J.; Burns, P. C. *J. Solid State Chem.* **2011**, *184* (7), 1591−1597.
(17) Arutyunyan, É. G.; Porai-Koshits, M. A.; Molodkin, A. K. *J. Struct. Chem.* **1966**, *7* (5), 683−686.
(18) Betke, U.; Wickleder, M. S. *Eur. J. Inorg. Chem.* **2012**, *2012* (2), 306−317.
(19) Habash, J.; Smith, A. J. *Acta Crystallogr.* **1983**, *C39*, 413−415.
(20) Habash, J.; Smith, A. J. *Acta Crystallogr.* **1990**, *C46*, 957−960.
(21) Habash, J.; Smith, A. J. *J. Cryst. Spectrosc. Res.* **1992**, *22* (1), 21−24.
(22) Knope, K. E.; Wilson, R. E.; Skanthakumar, S.; Soderholm, L. *Inorg. Chem.* **2011**, *50* (17), 8621−8629.
(23) Wilson, R. E.; Skanthakumar, S.; Knope, K. E.; Cahill, C. L.; Soderholm, L. *Inorg. Chem.* **2008**, *47* (20), 9321−9326.
(24) Charushnikova, I. A.; Krot, N. N.; Starikova, Z. A. *Radiochemistry* **1999**, *41* (2), 108−112.
(25) Charushnikova, I. A.; Krot, N. N.; Starikova, Z. A. *Radiochemistry* **2000**, *42* (1), 37−41.
(26) Charushnikova, I. A.; Krot, N. N.; Starikova, Z. A. *Radiochemistry* **2000**, *42* (1), 42−47.
(27) Charushnikova, I. A.; Krot, N. N.; Starikova, Z. A. *Radiochemistry* **2000**, *42* (5), 434−438.
(28) Jayadevan, N. C.; Mudher, K. D. S.; Chackraburtty, D. M. *Z. Kristallogr.* **1982**, *161* (1−2), 7−13.
(29) Kierkegaard, P. *Acta. Chem. Scan.* **1956**, *10* (4), 599−616.
(30) *Bruker APEX2 Software Suite, APEX2 v2011.4-1*; Bruker AXS: Madison, WI, 2011.
(31) Duvieubourg-Garela, L.; Vigier, N.; Abraham, F.; Grandjean, S. *J. Solid State Chem.* **2008**, *181* (8), 1899−1908.
(32) Zhang, Y.-J.; Collison, D.; Livens, F. R.; Powell, A. K.; Wocadlo, S.; Eccles, H. *Polyhedron* **2000**, *19* (14), 1757−1767.
(33) Spirlet, M. R.; Rebizant, J.; Kanellakopulos, B.; Dornberger, E. *Acta Crystallogr.* **1987**, *C43*, 19−21.
(34) Ruben, H. W.; Templeton, D. H.; Rosenstein, R. D.; Olovsson, I. *J. Am. Chem. Soc.* **1961**, *83* (4), 820−824.
(35) Zalkin, A.; Ruben, H. W.; Templeton, D. H. *Acta Crystallogr.* **1962**, *15*, 1219−1224.
(36) Zalkin, A.; Ruben, H. W.; Templeton, D. H. *Acta Crystallogr.* **1964**, *17*, 235−240.
(37) Haigh, C. W. *Polyhedron* **1995**, *14* (20−21), 2871−2878.
(38) Nyquist, R. A.; Putzig, C. L.; Leugers, M. A.; Kagel, R. O. *The Handbook of Infrared and Raman Spectra of Inorganic Compounds and Organic Salts: Infrared and Raman Spectral Atlas of Inorganic Compounds and Organic Salts. Text and Explanations*; Academic Press: San Diego, 1997; Vol. *1*.
(39) Nakamoto, K. *Infrared and Raman Spectra of Inorganic and Coordination Compounds Part A: Theory and Applications in Inorganic Chemistry*, 5th ed.; John Wiley & Sons, Inc.: New York, 1997.
(40) Lindgren, O. *Acta. Chem. Scand. A* **1977**, *31* (6), 453−456.
(41) Golovnya, V. A.; Bolotova, G. T. *Russ. J. Inorg. Chem.* **1961**, *6* (3), 288−292.